PERINATAL JOURNAL

Original Article

Perinatal Journal 2025; 33(1):926-935

https://doi.org/10.57239/prn.25.033100100

Suppression of wild-type EWSR1 enhances apoptosis and inhibits proliferation and inflammatory cytokine expression in activated hepatic stellate cells

Zhang Shiwan[1,2], Luo Guangcheng[3], Maisarah Binti Abdul Mutalib[2]*

[1]*Department of Infectious Diseases, Affiliated Hospital, Clinical Medical School, North Sichuan Medical College, Nanchong, Sichuan, China*
[2]*School of Graduate Studies, Postgraduate Centre, Management and Science University, Shah Alam, Selangor, Malaysia*
[3]*Department of Clinical Laboratory, Affiliated Hospital of North Sichuan Medical College, Nanchong, Sichuan, China*

Abstract

Hepatic stellate cells (HSCs) are central mediators of liver fibrosis, exhibiting enhanced proliferation, inflammatory signaling, and resistance to apoptosis upon activation. Ewing sarcoma breakpoint region 1 (EWSR1), an RNA-binding protein implicated in transcriptional regulation and cellular stress responses, has not been well studied in liver fibrogenesis. We aimed to investigate whether suppression of EWSR1 modulates apoptosis, proliferation, and inflammatory cytokine expression in activated HSCs. Human LX-2 cells were transfected with EWSR1-specific siRNAs and stimulated with TGF-β1 to induce activation. Apoptosis was evaluated using Annexin V/PI flow cytometry, TUNEL staining, and Western blotting of Bax, Bcl-2, Caspase-3, and cleaved Caspase-3. Proliferation was assessed by CCK-8 assay. Inflammatory cytokines (IL-1β, IL-6, TNF-α) were quantified at both mRNA and protein levels by qtr.-PCR and ELISA. Pearson correlation analyses were performed to examine the association between EWSR1 and inflammatory/apoptotic markers. EWSR1 knockdown significantly reduced IL-1β, IL-6, and TNF-α expression at both protein and mRNA levels. Apoptosis was enhanced, as shown by increased Annexin V/PI- and TUNEL-positive cells, upregulation of cleaved Caspase-3, and downregulation of Bax and Bcl-2. Cell proliferation was markedly suppressed following EWSR1 silencing. Correlation analysis revealed strong positive associations between EWSR1 and pro-inflammatory cytokines and apoptosis-resistance markers Bax and Bcl-2.

EWSR1 promotes proliferation, inflammation, and apoptosis resistance in activated HSCs. Its suppression enhances apoptosis and attenuates inflammatory cytokine expression, highlighting EWSR1 as a potential therapeutic target for liver fibrosis.

Keywords: EWSR1, RNA-binding proteins, Hepatic stellate cells, Liver fibrosis, Apoptosis, Proliferation, Inflammation

Introduction

Liver fibrosis, a reversible yet progressive wound-healing response to chronic hepatic injury, is primarily driven by the activation of HSCs, which transdifferentiate from vitamin A–storing perisinusoidal cells in the space of Disse into fibrogenic myofibroblast-like cells (Aydın & Akçalı, 2018). HSCs activation is a pivotal event in the progression of liver fibrosis.

Upon activation, HSCs secrete abundant extracellular matrix (ECM) proteins—including collagen I, fibronectin, and CTGF—leading to progressive deposition and liver scarring (Zhang et al., 2016).

Resistance to apoptosis is a hallmark of activated HSCs, allowing their persistence during fibrogenesis even after cessation of injurious stimuli (Aizawa et al., 2019). On the other hand, restoring apoptotic sensitivity in HSCs is a potential mechanism for fibrosis resolution, as demonstrated by numerous in vitro and in vivo studies.

Wild-type EWSR1 encodes a multifunctional RNA-binding protein that is widely expressed in normal tissues, where it plays important roles in transcriptional regulation, RNA processing, and stress responses. Unlike the oncogenic EWSR1 fusion proteins in sarcomas, wild-type EWSR1 participates in maintaining cellular homeostasis by modulating mRNA splicing, export, and stability (Hassoun, 2023). Recent evidence has begun to implicate EWSR1 in fibrotic processes: for instance, a matrine-derived compound (6 k) was shown to attenuate liver fibrosis by inhibiting EWSR1 function (Bao et al., 2023).

Based on its role in RNA metabolism and cellular stress adaptation, as well as recent research findings, EWSR1 is likely to affect the activation and survival of HSCs by regulating fibrotic signaling pathways such as TGF β/SMAD and oxidative stress. So we

Correspondence: Maisarah Binti Abdul Mutalib, Department of Clinical Laboratory, Affiliated Hospital of North Sichuan Medical College, Nanchong, Sichuan, China, **e-mail:** maisarah_abdulmutalib@msu.edu.my, **Received:** August 9, 2025 **Accepted:** October 6, 2025

hypothesized that suppression of EWSR1 in activated HSCs would enhance apoptosis, inhibit proliferation, and reduce the expression of pro-inflammatory cytokines—thus interrupting key fibrogenic mechanisms.

In this study, using TGF-β1–induced LX-2 cell activation as an in vitro model, we evaluated the effects of EWSR1 knockdown on apoptotic signaling (cleaved caspase-3, Bax/Bcl-2 ratio), cell proliferation, and inflammatory cytokine expression (IL-6, IL-1β). This work aims to elucidate the role of EWSR1 in HSCs survival and inflammatory response, providing new insights into its therapeutic potential for liver fibrosis.

Materials and Methods

Cell culture

The human hepatic stellate cell line LX-2 was obtained from [Baidi Cell Technology, China] and cultured in DMEM supplemented with 10% fetal bovine serum (FBS; Zhejiang Tianhang Biotechnology Co., Ltd., China) and 1% penicillin-streptomycin (Biotechnology, China) at 37°C in a humidified incubator with 5% CO_2.

EWSR1 siRNA transfection

Cells were seeded in 6-well plates at a density of 1–3 × 10^5 cells/well and cultured overnight. EWSR1-specific siRNAs (siRNA-1: 5′-AGCAGCTATGGACAGCAGAG-3′; siRNA-2: 5′-CAGCTACGGGCAGCAGAGTT-3′; siRNA-3: 5′-TATGGGCAGGAGTCTGGAGGA-3′) were synthesized by RiboBio (Guangzhou, China). Transfection was performed using Lipofectamine RNAiMAX reagent (Invitrogen, USA) according to the manufacturer's protocol. Briefly, 100 pmol of siRNA and 5 μL RNAiMAX were separately diluted in 100 μL Opti-MEM (Gibco, USA), mixed, incubated for 20 minutes at room temperature, and added to each well containing 1 mL Opti-MEM. After 24 hours, the transfection medium was replaced with fresh complete DMEM and continue to culture for 2-3 days.

TGF-β1 stimulation

To induce hepatic stellate cell activation, cells were treated with recombinant human TGF-β1 (MedChemExpress, USA) at a final concentration of 5 ng/mL for 24 hours following siRNA transfection.

Cell proliferation assay

Cell proliferation was evaluated using the M5 HiPer Cell Counting Kit (CCK-8; Polymer Biotech, China) according to the manufacturer's instructions. LX-2 cells were harvested by trypsinization and resuspended at a density of approximately 3×10^4 cells/mL. A total of 100 μL of cell suspension (approximately 3,000 cells per well) was seeded into 96-well plates.

After allowing cells to adhere in a humidified incubator at 37 °C for approximately 4 hours, treatments (such as siRNA transfection and TGF-β1 stimulation) were applied, and cells were incubated for 24–72 hours depending on the experimental design.

To assess proliferation, 10% CCK-8 reagent was freshly diluted in complete DMEM medium and added to each well to replace the old medium. Plates were returned to the incubator and incubated at 37 °C. The absorbance at 450 nm was measured every 15 minutes using a microplate reader (ELX800, Bio-Tek, USA), and the optimal time point was selected for final analysis.

Apoptosis analysis

Flow Cytometry using Annexin V-FITC/PI Apoptosis Detection Kit (BD Biosciences, USA). Cells were harvested, washed with cold PBS, stained according to kit instructions, and analyzed using a flow cytometer. Early and late apoptotic cells were quantified.

TUNEL Staining Apoptotic cells in paraffin-embedded liver tissues were detected using a TUNEL assay kit (Servicebio, China). Tissue sections were deparaffinized with xylene and rehydrated through graded ethanol. After washing with distilled water, sections were fixed in 4% paraformaldehyde for 20 minutes and rinsed with PBS. Permeabilization was performed using 0.1% Triton X-100 in PBS for 20 minutes at room temperature, followed by three PBS washes. Slides were then incubated with equilibration buffer for 10 minutes, and a freshly prepared TUNEL reaction mixture (TdT enzyme,

dUTP, buffer = 1:5:50) was added and incubated at 37 °C for 1 hour. After three PBS washes, nuclei were counterstained with DAPI for 10 minutes at room temperature in the dark. Slides were mounted with antifade mounting medium and visualized under a fluorescence microscope (Mingmei, China). TUNEL-positive cells showed red fluorescence, and DAPI-stained nuclei appeared blue.

Western blotting

Total proteins were extracted from LX-2 cells using RIPA lysis buffer (Zsbio, China) supplemented with PMSF (Sigma, China). Protein concentrations were determined using a BCA assay kit, and equal amounts of protein were subjected to SDS-PAGE, followed by transfer onto PVDF membranes. Membranes were blocked in 5% BSA (Zsbio, China) and incubated overnight at 4 °C with the following primary antibodies:

Caspase-3 (ab184787, Abcam, UK; 1:2000)

Cleaved Caspase-3 (ab32042, Abcam, UK; 1:500)

Bax (ab289364, Abcam, UK; 1:1000)

Bcl-2 (ab182858, Abcam, UK; 1:2000)

β-actin (81115-1-RR, Proteintech, USA; 1:5000)

After washing, membranes were incubated with HRP-conjugated secondary antibodies (ab6721, Abcam, UK or SE131, Solarbio, China; 1:2000) at 37 °C for 50 min. Bands were detected using enhanced chemiluminescence (ECL) reagents and imaged accordingly.

Quantitative real-time PCR

Total RNA was extracted from LX-2 cells using TRIzol reagent (Sigma, USA), followed by phase separation with chloroform, isopropanol precipitation, and washing with 75% ethanol. RNA pellets were dissolved in DEPC-treated water (Sigma, USA). Reverse transcription was carried out using the M5 First Strand cDNA Synthesis Kit (Mei5bio, China), and qPCR was performed using PerfectStart™ Green qPCR SuperMix (Mei5bio, China) on a Bio-Rad iQ5 Real-Time PCR System.

The reaction system (20 μL total volume) included 1 μL cDNA, 0.4 μL forward and reverse primers (10 μM), 10 μL qPCR SuperMix, and 8.2 μL nuclease-free water. Cycling conditions were as follows: 95 °C for 3 min; 40 cycles of 95 °C for 10 s and 55 °C for 30 s; followed by melt curve analysis.

Gene expression levels were normalized to β-actin and calculated using the 2^−ΔΔCt method. The primer sequences used were:

Table1. Primer sequences used for qPCR analysis

Gene	Forward Primer (5'-3')	Reverse Primer (5'-3')
β-actin	AGGAGAAGCTGTGCTACGTC	AATGCCAGGGTACATGGTGG
IL-6	TTCTCCACAATACCCCCAGGA	GGCATTTGTGGTTGGGTCAG
IL-1β	AACCTCTTCGAGGCACAAGG	AGATTCGTAGCTGGATGCCG
TNF-α	AGGGGCTGGTGAATATGTGC	TGGGAATTCCACCTTGGTCTG

ELISA assays for inflammatory factor

The concentrations of inflammatory cytokines in cell culture supernatants, including interleukin-1β (IL-1β), interleukin-6 (IL-6), and tumor necrosis factor-α (TNF-α), were measured using commercial ELISA kits according to the manufacturers' instructions. The IL-1β ELISA kit was purchased from Jianglai Bio (Shanghai, China), the IL-6 kit from Lianke Bio (Hangzhou, China), and the TNF-α kit from Pumoke (Wuhan) Biotechnology Co., Ltd (Wuhan, China). Absorbance was measured at 450 nm using a microplate reader (BioTek ELX800, USA), and cytokine concentrations were calculated based on standard curves.

Statistical analysis

All data are presented as mean ± standard deviation (SD) from at least three independent experiments. Statistical analysis was performed using *GraphPad Prism 9.0* and *SPSS21.0*. Quantitative data between groups were compared using *t-tests* or *one-way analysis of variance* (*ANOVA*). For post hoc comparisons following *ANOVA*, *Tukey's multiple comparisons test and Dunnett's multiple comparisons*

test were applied. *Pearson* correlation analysis was used to evaluate the relationships among biomarkers. A *p-value<0.05* was considered statistically significant.

Results

EWSR1 Inhibition reduces the expression of Pro-inflammatory cytokines in LX-2 cells

To investigate the effect of EWSR1 knockdown on the inflammatory response of HSCs, the expression levels of TNF-α, IL-6, and IL-1β were examined in Control, Model, and Model + si-EWSR1(3) groups. Cytokine levels were measured at both the protein level by ELISA and at the transcriptional level by qPCR.

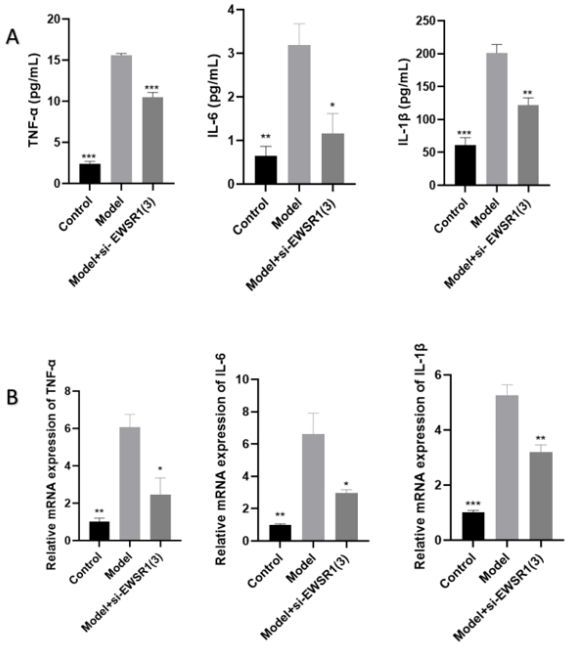

Figure1. EWSR1 knockdown suppresses the expression of pro-inflammatory cytokines in LX-2 cells

Expression levels of TNF-α, IL-6, and IL-1β were measured by ELISA and qRT-PCR in Control, Model (TGF-β1-treated), and Model + si-EWSR1(3) groups. Data are presented as mean±SD (n = 3). *p < 0.05, **p < 0.001, ***p < 0.0001 vs. Model group.

As shown in Figure 1A, ELISA results revealed that the expression of TNF-α was significantly reduced in the Control group (p<0.0001) and Model + si-EWSR1(3) group (p<0.0001) compared to the Model group, with significant differences among the three groups (F=890.591, p<0.0001). Similarly, IL-6 protein levels were markedly decreased in the Control group (p=0.0005) and si-EWSR1(3) group (p=0.0015) compared with the Model group (F=33.406, p=0.001). For IL-1β, both the Control (p<0.0001) and Model + si-EWSR1(3) (p=0.0003) groups showed significantly lower protein levels than the Model group, and the difference among groups was statistically significant (F=109.219, p<0.0001).

Consistent with protein level findings, qPCR results (Figure 1B) demonstrated that TNF-α mRNA expression was significantly decreased in the Control (p=0.0006) and si-EWSR1(3) groups (p=0.0029) compared to the Model group (F=37.602, p=0.001). IL-6 mRNA expression was also significantly lower in the Control (p=0.0002) and si-EWSR1(3) (p=0.0029) groups (F=41.666, p<0.0001). Similarly, IL-1β mRNA levels were significantly downregulated in the Control (p<0.0001) and si-EWSR1(3) groups (p=0.0002) compared with the Model group (F=185.329, p<0.0001). These results indicate that EWSR1 knockdown significantly suppresses the expression of pro-inflammatory cytokines at both the mRNA and protein levels in activated LX-2 cells.

EWSR1 knockdown promotes apoptosis in activated LX-2 cells

To investigate the effect of EWSR1 inhibition on apoptosis in hepatic stellate cells, we assessed the expression of apoptosis-related proteins Bax, Bcl-2, Caspase-3, and Cleaved-Caspase-3 (C-caspase3) in Control, Model, and Model + si-EWSR1(3) groups using Western blot analysis. In addition, TUNEL staining and Annexin V-FITC/PI flow cytometry were performed to evaluate DNA fragmentation and apoptotic rates.

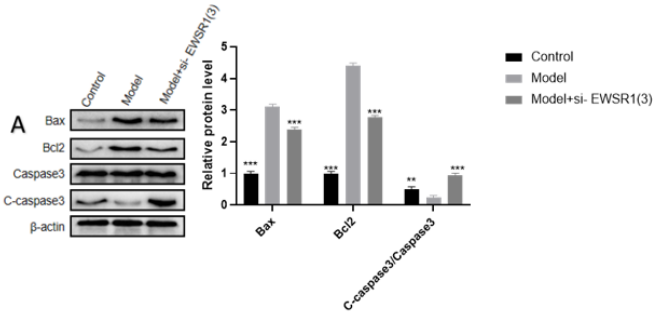

Figure 2. (A) EWSR1 knockdown promotes apoptosis in activated LX-2 cells

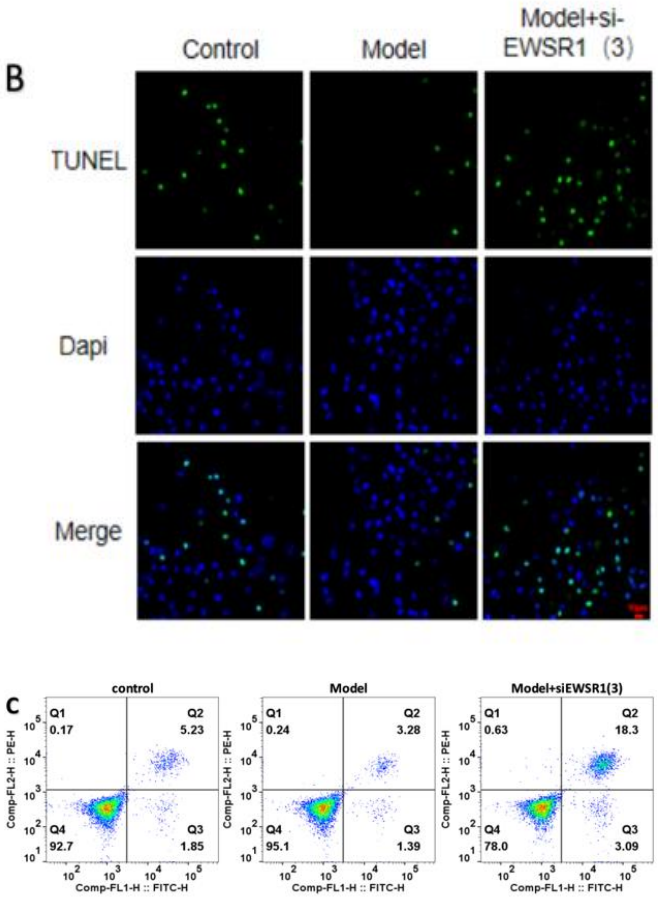

Figure 2. EWSR1 knockdown promotes apoptosis in activated LX-2 cells.

(A) Western blot analysis of apoptosis-related proteins Bax, Bcl-2, Caspase-3, and C-caspase3 in Control, Model, and Model + si-EWSR1(3) groups. Protein levels were normalized to β-actin. Quantification of relative protein expression is shown above.
(B) TUNEL assay was performed to detect DNA fragmentation in each group. TUNEL-positive cells (green) indicate apoptotic cells, and nuclei were counterstained with DAPI (blue). EWSR1 knockdown increased TUNEL positivity in activated LX-2 cells. Scale bar = 20 μm.
(C) Flow cytometric analysis of apoptosis using Annexin V-FITC/PI staining. The percentage of apoptotic cells (early apoptosis: Q3; late apoptosis: Q2) increased significantly in the Model + si-EWSR1(3) group compared to the Model group. Data are presented as mean ± SD (n=3). *p<0.05, **p<0.001, ***p<0.0001 vs. Model group.

As shown in Figure 2A, Western blot results revealed that Bax protein expression was significantly upregulated in the Model ($p<0.0001$) compared to the Control group. Bax expression in the si-EWSR1(3) group was significantly lower than in the Model group ($p<0.0001$), with an overall group difference confirmed by ANOVA ($F=703.887$, $p<0.0001$). Bcl-2, an anti-apoptotic protein, was also significantly increased in the Model ($p<0.0001$) compared to Control, and si-EWSR1(3) treatment significantly reduced Bcl-2 expression compared with the Model group ($p<0.0001$); The comparison between the three groups was significant ($F=1777.154$, $p=0.000$);

Furthermore, the ratio of C-Caspase-3 to total Caspase-3 (C-caspase3/Caspase3) was significantly increased in the Model + si-EWSR1(3) group compared to Model group ($p<0.0001$) indicating reactivation of caspase-dependent apoptosis. The differences among groups were statistically significant ($F=75.633$, $p<0.0001$).

TUNEL staining results (Figure 2B) showed few apoptotic cells in the Control and Model groups, while a notable increase in TUNEL-positive cells was observed in the Model + si-EWSR1(3) group, indicating enhanced DNA fragmentation and nuclear condensation upon EWSR1 knockdown.

Flow cytometric analysis (Figure 2C) further confirmed the pro-apoptotic effect of EWSR1 inhibition. The percentage of apoptotic cells (Q2 + Q3 quadrants) increased markedly in the si-EWSR1(3) group (early apoptosis: 3.09%, late apoptosis: 18.3%) compared to the Model group (1.39% and 3.28%, respectively) and Control group (1.85% and 5.23%).

These results demonstrate that EWSR1 knockdown promotes apoptosis in activated LX-2 cells, potentially through modulation of mitochondrial apoptotic signaling and caspase activation.

3. EWSR1 Knockdown Inhibits Cell Proliferation in Activated LX-2 Cells

To evaluate the impact of EWSR1 on hepatic stellate cell proliferation, the CCK-8 assay was used to assess cell viability among Control, Model, and Model + si-EWSR1(3) groups.

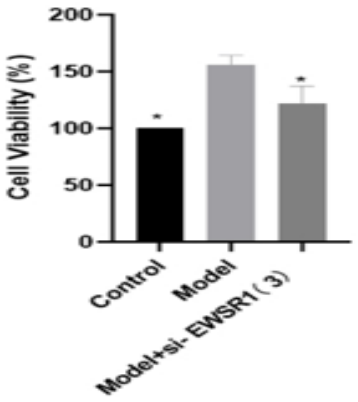

Figure 3. EWSR1 knockdown reduces cell proliferation in activated LX-2 cells

Cell proliferation was assessed by Cell Counting Kit-8 (CCK-8) assay in Control, Model (TGF-β1-treated), and Model + si-EWSR1(3) groups. Compared with the Model group, cell viability was significantly reduced in the Control and Model + si-EWSR1(3) groups. Data are presented as mean ± SD (n = 3). *p < 0.05 vs. Model group. WSR1 Knockdown Inhibits Cell Proliferation in Activated LX-2 Cells

As shown in Figure 3, cell proliferation was significantly increased in the Model group compared to the Control group (p = 0.0011), indicating successful activation of LX-2 cells by TGF-β1. In contrast, EWSR1 knockdown significantly suppressed cell proliferation. The absorbance values in the Model + si-EWSR1(3) group were significantly lower than those in the Model group (p = 0.0139). One-way ANOVA indicated that the differences among the three groups were statistically significant (F=24.371, p=0.001). These findings suggest that EWSR1 plays a role in promoting the proliferative phenotype of activated LX-2 cells.

Correlation analysis between EWSR1 and apoptosis markers, inflammatory factors

To further investigate the relationship between EWSR1 and inflammatory factors (IL-1β, IL-6, TNF-α), apoptosis-related proteins (Bax, Bcl2 and C-caspase3. Pearson correlation analysis was performed. EWSR1 expression exhibited strong positive correlations with pro-inflammatory cytokines IL-1β (r=0.976, p<0.05), IL-6 (r=0.930, p<0.05), and TNF-α (r=0.876, p<0.05). In addition, EWSR1 expression was positively correlated with both Bax (r =0.992, p < 0.05) and Bcl-2 (r=0.986, p<0.05). Conversely, a significant negative correlation was observed between EWSR1 and C-caspase3 (r=-0.245, p<0.05). These findings suggest that high EWSR1 expression is associated with a pro-inflammatory and apoptosis-resistant phenotype in activated HSCs.

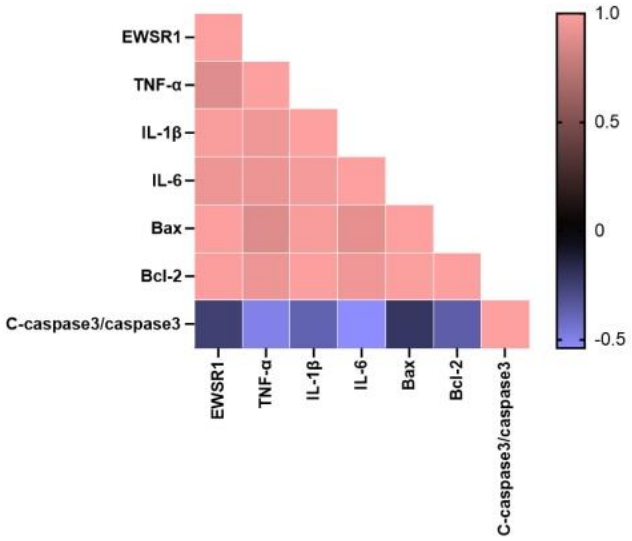

Figure 4. Correlation heatmap between EWSR1 and apoptosis markers, inflammatory factors

Correlation heatmap of EWSR1 expression with inflammatory cytokines and apoptosis markers in Control, Model, and Model + si-EWSR1(3) groups. Pearson correlation coefficients are represented by color intensity, with red indicating positive correlation and blue indicating negative correlation. EWSR1 showed strong positive correlations with IL-1β, IL-6, TNF-α, Bax, and Bcl-2, and a negative correlation with C-caspase3, suggesting that EWSR1 expression is closely linked to the inflammatory and apoptotic phenotype of activated HSCs.

Discussion

Liver fibrosis is a common pathological endpoint of chronic liver injuries such as viral hepatitis, alcohol abuse, and non-alcoholic steatohepatitis (NASH), characterized by hepatocyte damage, inflammatory cytokine release, and fibrotic remodeling of the liver parenchyma (Henderson et al., 2020). HSCs are central to this process, transitioning from a quiescent vitamin A–storing phenotype to a highly proliferative,

fibrogenic, and inflammation-amplifying state upon exposure to persistent injury cues (Tsuchida & Friedman, 2017). During activation, HSCs not only produce excessive extracellular matrix components but also resist apoptosis and secrete various pro-inflammatory cytokines such as IL-1β, IL-6, and TNF-α, thereby perpetuating liver injury and fibrosis (Garbuzenko, 2022).

Apoptosis resistance and chronic inflammation are thus considered hallmarks of activated HSCs, contributing to their prolonged survival and profibrotic activity in the damaged liver microenvironment (Akkiz et al., 2024). In recent years, attention has turned to regulatory proteins that integrate signals from stress, inflammation, and survival pathways. Among these, the Ewing sarcoma breakpoint region 1 (EWSR1) gene, which encodes a multifunctional RNA-binding protein, has emerged as a key modulator of gene transcription, mRNA stability, and stress responses (Jiang et al., 2021).

Although best known for its oncogenic fusions in sarcoma, wild-type EWSR1 has also been implicated in apoptosis resistance and inflammation regulation in non-cancerous contexts (Bao et al., 2023). However, its role in hepatic fibrogenesis has remained unclear. Given its involvement in transcriptional control and its potential to interact with stress-responsive factors such as p53 and NF-κB(Li & Chen, 2022), we hypothesized that EWSR1 may contribute to the anti-apoptotic and pro-inflammatory phenotype of activated HSCs.

In this study, we therefore investigated the effects of EWSR1 silencing on apoptosis induction, cell proliferation, and inflammatory cytokine expression in TGF-β1–activated LX-2 cells. By targeting EWSR1, we aimed to determine whether its suppression could restore apoptotic sensitivity and dampen the inflammatory response in activated HSCs—thus providing mechanistic insights and potential therapeutic value for reversing liver fibrosis.

Previous studies have already implicated EWSR1 in transcriptional regulation, RNA metabolism, and stress granule formation, all of which may influence inflammatory signaling pathways. For instance, the EWSR1–ATF1 fusion protein has been associated with elevated IL-6 expression in angiomatoid fibrous histiocytoma, implicating EWSR1's involvement in IL-6–mediated inflammatory regulation (Eberst et al., 2020), This suggests that EWSR1 may modulate cytokine pathways in non-malignant contexts as well.

Our results demonstrated that EWSR1 inhibition significantly attenuated the expression of pro-inflammatory cytokines TNF-α, IL-6, and IL-1β in TGF-β1-activated LX-2 cells. Both mRNA and protein levels of these cytokines were markedly increased in the fibrotic model group, while siRNA-mediated knockdown of EWSR1 led to a substantial reduction in their expression. These findings suggest that EWSR1 may act as a positive regulator of the inflammatory microenvironment during HSCs activation.

The pro-fibrotic activation of HSCs is not only associated with excessive ECM production but also accompanied by a pro-inflammatory phenotype, which contributes to further paracrine activation of neighboring cells and the perpetuation of fibrosis. TNF-α and IL-1β are classical pro-inflammatory cytokines that promote HSCs activation, survival, and collagen synthesis (Das & Medhi, 2023), while IL-6 has been shown to enhance HSCs proliferation and resistance to apoptosis (Hou et al., 2014). The downregulation of these cytokines following EWSR1 knockdown indicates that EWSR1 may participate in upstream regulatory events controlling the inflammatory status of HSCs. our data reveal a novel role for EWSR1 in maintaining the inflammatory phenotype of activated HSCs, and suggest that its inhibition may have therapeutic potential in reducing inflammation-driven fibrogenesis.

Apoptosis resistance is a key feature of activated HSCs, allowing them to maintain ECM production and promote fibrosis even after the removal of fibrogenic stimuli. The Bcl-2 family proteins regulate the mitochondrial apoptotic pathway, with Bax promoting apoptosis and Bcl-2 exerting anti-apoptotic effects (Qian et al., 2022). Prevoius study has shown that zebrafish embryos lacking EWSR1 orthologues exhibit p53-mediated apoptotic death, underscoring a conserved role in cell survival (Azuma et al., 2007).

In this study, we also observed that EWSR1 knockdown significantly promoted apoptosis in TGF-β1–activated LX-2 cells. Notably, while both Bax and Bcl-2 protein levels were decreased in the si-

EWSR1(3) group compared to the model group, the ratio of cleaved-Caspase-3 to total Caspase-3 was markedly increased. Caspase-3 is a central executioner caspase that exists in its inactive zymogen form (pro-Caspase-3) and must be proteolytically cleaved into cleaved-Caspase-3 to execute apoptosis. Therefore, an elevated cleaved-Caspase-3/Caspase-3 ratio indicates enhanced activation of the apoptotic machinery, even in the context of reduced total Caspase-3 expression. Classical mitochondrial pathways would predict Bax upregulation alongside Bcl-2 downregulation during apoptosis, our data show simultaneous decreases in both, suggesting that EWSR1 suppression initiates the mitochondrial apoptosis pathway, even in a Bax-independent manner.

These molecular changes were corroborated by both TUNEL staining and Annexin V-FITC/PI flow cytometry, which showed significantly increased apoptotic cell populations in the si-EWSR1(3) group. Therefore, these findings indicate that EWSR1 may exert an anti-apoptotic effect in activated HSCs, its inhibition can promote the apoptosis of HSCs and help reverse the fibrosis process by activating Caspase-3 and inducing Bax non-dependent mitochondrial apoptosis pathway.

Although the precise mechanism remains to be fully defined, EWSR1 has been shown in other cell types to interact with apoptosis regulators such as p53, caspase components, or stress granule-associated pathways. Whether similar mechanisms are involved in HSCs requires further investigation. Overall, our findings indicate that EWSR1 inhibition may facilitate the resolution of fibrosis by promoting apoptosis of myofibroblast-like cells.

Our results further revealed that EWSR1 knockdown suppressed the proliferative activity of LX-2 cells under fibrogenic conditions. The CCK-8 assay showed a significant increase in cell viability upon TGF-β1 stimulation, reflecting the activation and proliferative response of HSCs. Silencing EWSR1 led to a marked reduction in cell proliferation, indicating that EWSR1 may contribute to the maintenance of the activated and proliferative phenotype of HSCs.

Proliferation of HSCs is a critical component of liver fibrogenesis. Once activated, HSCs not only produce extracellular matrix components but also undergo rapid clonal expansion, contributing to the progression and persistence of fibrosis. The observed decrease in proliferation following EWSR1 knockdown suggests that EWSR1 may regulate cell cycle progression, survival signaling, or growth factor responsiveness in activated HSCs.

Although there are limited direct studies on wild-type EWSR1 in HSCs, literature from Ewing sarcoma and other tumor models indicates that EWSR1–fusion proteins profoundly impact cell cycle regulation and proliferation via modulation of cyclins, CDKs, MYC transcription, and RNA splicing machinery (Kowalewski et al., 2011). For instance, EWSR1:WT1 fusion upregulates the cyclin D-CDK4/6 RB signaling axis in fibromatoid small round cell tumors, and CDK4/6 inhibitors can reverse its proliferative promoting effect (Magrath et al., 2024). Besides, EWSR1: CREAM fusion knockdown can alter the expression of a variety of cell proliferation-related genes and affect cell migration ability (Kaprio et al., 2023).

With our apoptosis data, the reduction in cell proliferation reinforces the hypothesis that EWSR1 supports the survival and expansion of activated HSCs. Its inhibition not only promotes apoptosis but also suppresses mitogenic activity, providing a dual mechanism for its potential antifibrotic effects.

Our correlation analysis revealed that EWSR1 expression correlates positively with pro-inflammatory cytokines (IL-1β, IL-6, TNF-α) and anti-apoptotic protein Bcl-2, but negatively with cleaved caspase-3, indicating that high EWSR1 levels are closely associated with both inflammatory activation and apoptosis resistance in activated hepatic stellate cells.

EWSR1 has not previously been linked directly to this integrated inflammatory-anti-apoptotic network in HSCs. However, its known functions as an RNA-binding and transcriptional regulator in other cell types suggesting a plausible mechanistic basis.

Taken together, our data position wild-type EWSR1 as a potential central regulator in activated HSCs, integrating pro-inflammatory cytokine expression with anti-apoptotic mechanisms. Its inhibition appears to disrupt this coordinated network—dampening inflammation while enabling apoptotic

resolution—thus offering a dual antifibrotic strategy. These insights pave the way for further investigation into EWSR1's direct molecular targets—such as whether it stabilizes mRNAs encoding inflammatory cytokines or pro-survival factors.

Conclusion

EWSR1 silencing significantly enhances apoptosis, reduces inflammation, and suppresses proliferation in activated hepatic stellate cells. These findings suggest that EWSR1 inhibition exerts dual antifibrotic effects—suppressing inflammatory activation while promoting the apoptotic clearance of activated HSCs. Given these results, wild-type EWSR1 emerges as a promising therapeutic target for liver fibrosis, warranting further mechanistic investigation and in vivo validation.

Data availability statement

Data and materials will be made available on request.

Author contributions

Zhang Shiwan: Conceptualization, Methodology, Investigation, Data Curation, Formal Analysis, Writing-Original Draft. Luo Guangcheng: Conceptualization, Supervision, Writing-Review & Editing, Corresponding Author. Maisarah Binti Abdul Mutalib: Conceptualization, Supervision, Writing-Review & Editing, Corresponding Author.

Acknowledgments

The authors thank the members of our department and laboratory for their support and technical help.

Conflicts of interest

The authors have no conflicts to report.

References

Aizawa, S., Brar, G., Tsukamoto, H. J. G., & liver. (2019). Cell death and liver disease. *14*(1), 20.

Akkiz, H., Gieseler, R. K., & Canbay, A. (2024). Liver Fibrosis: From Basic Science towards Clinical Progress, Focusing on the Central Role of Hepatic Stellate Cells. *Int J Mol Sci*, *25*(14). https://doi.org/10.3390/ijms25147873

Aydın, M. M., & Akçalı, K. C. (2018). Liver fibrosis. *The Turkish Journal of Gastroenterology*, *29*(1), 14.

Azuma, M., Embree, L. J., Sabaawy, H., & Hickstein, D. D. (2007). Ewing sarcoma protein ewsr1 maintains mitotic integrity and proneural cell survival in the zebrafish embryo. *PLoS One*, *2*(10), e979.

Bao, Y., Niu, T., Zhu, J., Mei, Y., Shi, Y., Meng, R.,…Wang, Y. (2023). Evolution and Discovery of Matrine Derivatives as a New Class of Anti-Hepatic Fibrosis Agents Targeting Ewing Sarcoma Breakpoint Region 1 (EWSR1). *Journal of Medicinal Chemistry*, *66*(12), 7969-7987.

Das, P. P., & Medhi, S. J. C. (2023). Role of inflammasomes and cytokines in immune dysfunction of liver cirrhosis. *170*, 156347.

Eberst, L., Cassier, P. A., Brahmi, M., Tirode, F., & Blay, J.-Y. J. E. o. (2020). Tocilizumab for the treatment of paraneoplastic inflammatory syndrome associated with angiomatoid fibrous histiocytoma. *5*(3).

Garbuzenko, D. V. (2022). Pathophysiological mechanisms of hepatic stellate cells activation in liver fibrosis. *World Journal of Clinical Cases*, *10*(12), 3662.

Hassoun, Z. E. O. (2023). *A Novel Role of EWSR1 Protein in RNA Translation Regulation* (Doctoral dissertation,Universite de Liege (Belgium))].

Henderson, N. C., Rieder, F., & Wynn, T. A. (2020). Fibrosis: from mechanisms to medicines. *Nature*, *587*(7835), 555-566. https://doi.org/10.1038/s41586-020-2938-9

Hou, W., Jin, Y.-H., Kang, H. S., & Kim, B. S. J. J. o. v. (2014). Interleukin-6 (IL-6) and IL-17 synergistically promote viral persistence by inhibiting cellular apoptosis and cytotoxic T cell function. *88*(15), 8479-8489.

Jiang, W., Wu, T., Shi, X., & Xu, J. J. B. (2021). Overexpression of EWSR1 (Ewing sarcoma breakpoint region 1/EWS RNA binding protein 1) predicts poor survival in patients with hepatocellular carcinoma. *12*(1), 7941-7949.

Kaprio, H., Siddiqui, A., Saustila, L., Heuser, V. D., & Gardberg, M. J. S. R. (2023). The oncogenic properties of the EWSR1:: CREM fusion gene are associated with polyamine metabolism. *13*(1), 4884.

Kowalewski, A. A., Randall, R. L., & Lessnick, S. L. J. S. (2011). Cell Cycle Deregulation in Ewing′ s

Sarcoma Pathogenesis. *2011*(1), 598704.

Li, M., & Chen, C. J. C. (2022). Regulation of metastasis in Ewing sarcoma. *14*(19), 4902.

Magrath, J. W., Sampath, S. S., Flinchum, D. A., Hartono, A. B., Goldberg, I. N., Boehling, J. R.,…Lee, S. B. J. C. R. (2024). Comprehensive transcriptomic analysis of EWSR1:: WT1 targets identifies CDK4/6 inhibitors as an effective therapy for desmoplastic small round cell tumors. *84*(9), 1426-1442.

Qian, S., Wei, Z., Yang, W., Huang, J., Yang, Y., & Wang, J. J. F. i. o. (2022). The role of BCL-2 family proteins in regulating apoptosis and cancer therapy. *12*, 985363.

Tsuchida, T., & Friedman, S. L. (2017). Mechanisms of hepatic stellate cell activation. *Nature reviews Gastroenterology & hepatology*, *14*(7), 397-411.

Zhang, C.-Y., Yuan, W.-G., He, P., Lei, J.-H., & Wang, C.-X. J. W. j. o. g. (2016). Liver fibrosis and hepatic stellate cells: Etiology, pathological hallmarks and therapeutic targets. *22*(48), 10512.